

A unique Neutrino Mass Matrix Texture under Exponential Parametrization

Pralay Chakraborty^a, Subhankar Roy^{a,*}

^a*Department of Physics, Gauhati University, India*

Abstract

Under the exponential parametrization scheme $m_{ij}^\nu \sim r e^{i\theta}$, we propose a *unique* neutrino mass matrix texture that exhibits four correlations among its elements. The mixing scheme obtained from the proposed texture is consistent with experimental observations. We construct a concrete model based on the $SU(2)_L \times U(1)_Y \times A_4 \times Z_{10}$ group within the framework of the seesaw mechanism.

1. Introduction

The neutrino oscillation suggests that neutrinos change their identity as they traverse space [1]. This phenomenon can be understood from the quantum mechanics framework which tells us that the three flavour states of neutrinos ($\nu_{l=e,\mu,\tau}$) are the mixture of three mass eigenstates ($\nu_{i=1,2,3}$) having definite masses ($m_{i=1,2,3}$). The neutrino oscillation predicts the existence of non-zero mass, which goes against the predictions of the Standard Model (SM) [2, 3, 4]. In this regard, we need to go beyond the SM framework to understand the non-zero neutrino masses. The neutrino mass matrix (M_ν) originates from the Yukawa Lagrangian, which can be understood from the see-saw mechanism [5, 6, 7, 8, 9, 10, 11, 12, 13]. In general, a Majorana neutrino mass matrix contains the information of twelve parameters: three mass eigenvalues ($m_{i=1,2,3}$), three mixing angles ($\theta_{12}, \theta_{13}, \theta_{23}$), three CP phases (δ, α, β), and three unphysical phases (ϕ_1, ϕ_2, ϕ_3). Recent experiments predict three mixing angles and two mass-squared differences (Δm_{21}^2 and Δm_{31}^2) precisely [14]. However, the octant of θ_{23} , neutrino mass ordering and a precise bound of δ are yet to be determined. In addition, the oscillation experiments do not measure three individual mass eigenvalues and the Majorana phases.

However, the M_ν carries the information of all nine physical parameters, and by imposing certain constraints on M_ν , some of the physical parameters can be predicted. Various constraints, such as texture zeroes [15], vanishing minors [16], hybrid textures [17], and $\mu - \tau$ symmetry [18] are widely studied in the literature. The experiments rule out the $\mu - \tau$ symmetry due to its prediction of θ_{13} being zero. In this regard, there are several attempts made to explore deviations from the exact $\mu - \tau$ symmetry [19, 20, 21]. In the present work, we explore different types of constraints, deviating from the existing literature. We adhere to the exponential parametrization of the neutrino mass matrix $M_{\nu_{ij}} = r_{ij} e^{i\theta_{ij}}$, where, r_{ij} represents the absolute value and θ stands for argument of the matrix elements. In contrast, a complex number z can also be expressed as $z = x + iy$. In principle, physics is independent of parametrization. The underlying principles and phenomena do not alter regardless of the parametrization we choose. However, a suitable parametrization may lead to understand the underlying physics in a better way. Like several other constraints studied in the literature, the said parametrization scheme offers new insights into how physical parameters can be correlated in a different way. The idea of the said parametrization was first discussed in a model-independent way in Ref [22]. The latter discusses several promising textures from different categories, highlighting distinct correlations including the exponential parametrization. All the proposed textures are experimentally viable. However, we have not provided any concrete model in support of the said textures.

In the present work, we put forward a *unique* texture for the neutrino mass matrix highlighting four correlations among the parameters under exponential parametrization, thereby predicting four physical parameters. In addition, following a top-down approach, we derive the texture in its *exact form*, ensuring that the independence of the texture parameters is preserved.

The plan of the paper is outlined as follows: In section (2), we discuss the details of the proposed texture. In section (3), we discuss the applications. Section (4) is devoted to the symmetry realization. In section (5), we conclude.

*Corresponding author

Email addresses: pralay@gauhati.ac.in (Pralay Chakraborty), subhankar@gauhati.ac.in (Subhankar Roy)

2. Formalism

In the present work, we stick to the Majorana nature of neutrino and hence the neutrino mass matrix is expected to be symmetric. In the light of the exponential parametrization, the neutrino mass matrix appears as: $M_{\nu_{ij}} = |m_{ij}| e^{i\theta_{ij}}$.

Following the said parametrization, we shall try to find out some correlations among the absolute and argument parts of the different matrix elements in a model independent way, which are promising from the phenomenological perspective.

2.1. The Proposed Texture

We posit the following neutrino mass matrix,

$$M_\nu = \begin{bmatrix} A & \mathbf{r}e^{i\theta} & \mathbf{r}e^{-i\theta} \\ \mathbf{r}e^{i\theta} & F & G \\ \mathbf{r}e^{-i\theta} & G & 2\mathbf{r}e^{i\theta} \end{bmatrix}, \quad (1)$$

where, A , F and G are complex parameters. Here, the parameters A , F and G are not highlighted in polar form as the correlations among these elements are not sought out. As the above texture showcases four independent correlations, hence we expect four observables to be predicted.

To draw information on the physical parameters, we need to diagonalize $M : M^d = V^T M V$, where, V is a 3×3 unitary matrix known as Pontecorvo-Maki-Nakagawa-Sakata (PMNS) matrix [23]. In general, the PMNS matrix is defined in flavour basis i.e., the basis where the charged lepton mass matrix is diagonal. The Particle Data Group (PDG) [24] has adopted a parametrization for V , where, V is parametrized using three angles and six phases as shown below,

$$V = P_\phi \cdot U \cdot P_M,$$

where, $P_\phi = \text{diag}(e^{i\phi_1}, e^{i\phi_2}, e^{i\phi_3})$ and $P_M = \text{diag}(e^{i\alpha}, e^{i\beta}, 1)$. The matrix U is depicted as shown in the following,

$$U = \begin{bmatrix} 1 & 0 & 0 \\ 0 & c_{23} & s_{23} \\ 0 & -s_{23} & c_{23} \end{bmatrix} \times \begin{bmatrix} c_{13} & 0 & s_{13} e^{-i\delta} \\ 0 & 1 & 0 \\ -s_{13} e^{i\delta} & 0 & c_{13} \end{bmatrix} \times \begin{bmatrix} c_{12} & s_{12} & 0 \\ -s_{12} & c_{12} & 0 \\ 0 & 0 & 1 \end{bmatrix},$$

where, $s_{ij} = \sin \theta_{ij}$ and $c_{ij} = \cos \theta_{ij}$.

In the present work, we assume that the unphysical phases $\phi_i = 1, 2, 3$ are excluded by redefining the charged lepton fields. In the next section, we shall discuss the experimental viability of the proposed texture.

2.2. Numerical Analysis

The four correlations appearing in M_ν of Eq. (1), are manifested as four transcendental equations involving nine physical parameters: $f_i(\theta_{12}, \theta_{13}, \theta_{23}, m_1, m_2, m_3, \delta, \alpha, \beta) = 0$, where, $i = 1, 2, 3, 4$. We solve these equations by the Newton-Raphson method to generate a sufficient number of random numbers for the parameters α , β , δ and θ_{23} . For this, we set the mixing angles θ_{12} and θ_{13} at their respective 3σ bound. The mass eigenvalues m_1 , m_2 and m_3 are estimated from two mass squared differences Δm_{21}^2 and Δm_{31}^2 , such that Σm_i is consistent with the cosmological data [25].

The analysis leads to some interesting predictions of the observable parameters. We see that θ_{23} lies within 42° to 47° approximately (within the 3σ range [14]). The δ experiences two narrow bounds: 5.43° - 12.32° ; and 347.52° - 354.52° . Thus, we see that within the allowed 3σ bound for δ given by the experiments, the above texture defines a forbidden region also. Similarly, we see that the Majorana phases α and β have got two and four allowed bounds respectively. We see, $\alpha \sim 85.37^\circ - 94.66^\circ, 265.33^\circ - 274.68^\circ$; and $\beta \sim 77.32^\circ - 80.33^\circ, 99.09.33^\circ - 102.78^\circ, 257.35^\circ - 260.74^\circ, 279.14^\circ - 282.72^\circ$. For a better visualisation of the allowed and forbidden regions of the predicted parameters, we refer to Fig. (1).

Though the mass parameters are taken as input, yet a graphical visualisation of the mass spectra is put forward in Fig. (2(a)). In addition, we generate the correlation plots to visualize the predictions of the studied parameters (see Figs. (2(b))-(2(d))). We know that the Jarlskog invariant (J_{CP}) [26], that represents the amount of the leptonic CP violation can be obtained in terms of standard parametrization as shown below,

$$J_{CP} = s_{13} c_{13}^2 s_{12} c_{12} s_{23} c_{23} \sin \delta.$$

In this regard, we visualize the variation of J_{CP} against Dirac CP phase δ from the proposed texture (see Fig. 2(e)). The maximum and minimum values of the studied parameters are listed in Table (1).

It is important to mention that the proposed texture is valid only for the normal ordering of neutrino masses. For inverted ordering, the texture is ruled out as the prediction of θ_{23} goes outside the experimental bound.

In the next section, we shall try to analyse the viability of the above texture in the light of other physical parameters.

Parameters	Texture Prediction (Min Value)	Texture Prediction (Max Value)	Model Prediction (Min Value)	Model Prediction (Max Value)
m_1/eV	0.017	0.029	0.017	0.029
m_2/eV	0.019	0.031	0.019	0.031
m_3/eV	0.052	0.058	0.053	0.059
$\sum m_i/\text{eV}$	0.09	0.118	0.09	0.119
$\theta_{23}/^\circ$	42.17	47.61	42.19	47.47
$\delta/^\circ$	5.43	354.52	5.67	353.83
$\alpha/^\circ$	85.37	274.68	85.53	274.56
$\beta/^\circ$	77.32	282.72	77.36	282.59
$m_{\beta\beta}/\text{meV}$	16.10	28.43	16.16	28.21

Table 1: Shows the maximum and minimum values of m_1 , m_2 , m_3 , $\sum m_i$, θ_{23} , δ , α , β and $m_{\beta\beta}$.

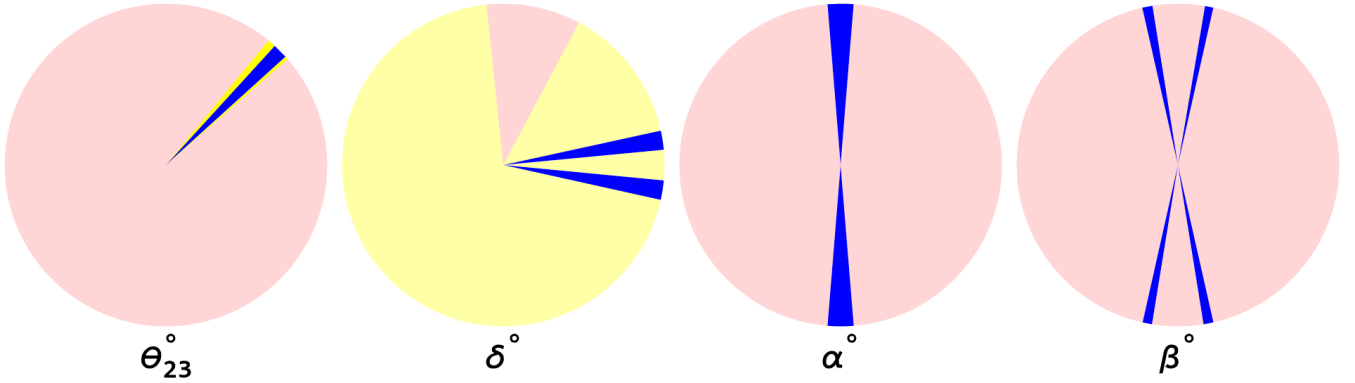


Figure 1: The allowed and forbidden regions for the physical parameter based on texture predictions. The blue region signifies the allowed region and yellow region stands for 3σ region for the studied parameters.

3. Applications

In the earlier section, the proposed texture is found to be consistent with the neutrino oscillation experiments. However, the viability of the texture can be further tested in the light of other physical observables.

3.1. Effective Majorana Neutrino Mass

The neutrino-less double beta decay ($0\nu\beta\beta$) [27], is a lepton number violating decay. Its discovery would justify the Majorana nature of neutrinos. The decay rate Γ is determined by the phase space factor $G^{0\nu}$, the nuclear matrix element $M^{0\nu}$, and the effective Majorana mass $m_{\beta\beta}$, following the relation: $\Gamma \sim G^{0\nu} \cdot M^{0\nu} \cdot m_{\beta\beta}^2$.

The effective Majorana neutrino mass $m_{\beta\beta}$ is an observational parameter and it can be expressed as:

$$m_{\beta\beta} = \left| \sum_{k=1}^3 U_{1k}^2 m_k \right|.$$

where, m_1 , m_2 and m_3 are the three mass eigenvalues. The U_{11} , U_{12} and U_{13} are the elements of the PMNS matrix that contains the information of α and β . Several experiments have provided the upper bounds of $m_{\beta\beta}$: SuperNEMO(Se⁸²) as 67 – 131 meV, GERDA(Ge⁷⁶) as 104 – 228 meV, EXO-200(Xe¹³⁶) as 111 – 477 meV, CUORE(Te¹³⁰) as 75 – 350 meV and KamLAND-Zen(Xe¹³⁶) as 61 – 165 meV [28, 29, 30, 31, 32, 33, 34]. In this regard, we visualize the prediction of the parameter $m_{\beta\beta}$ from the proposed texture (see Fig. 2(f)). It is important to mention that the prediction of $m_{\beta\beta}$ from the proposed texture (16.10 – 28.43) meV partially falls within the sensitivity of future experiments such as LEGEND-1000 [35].

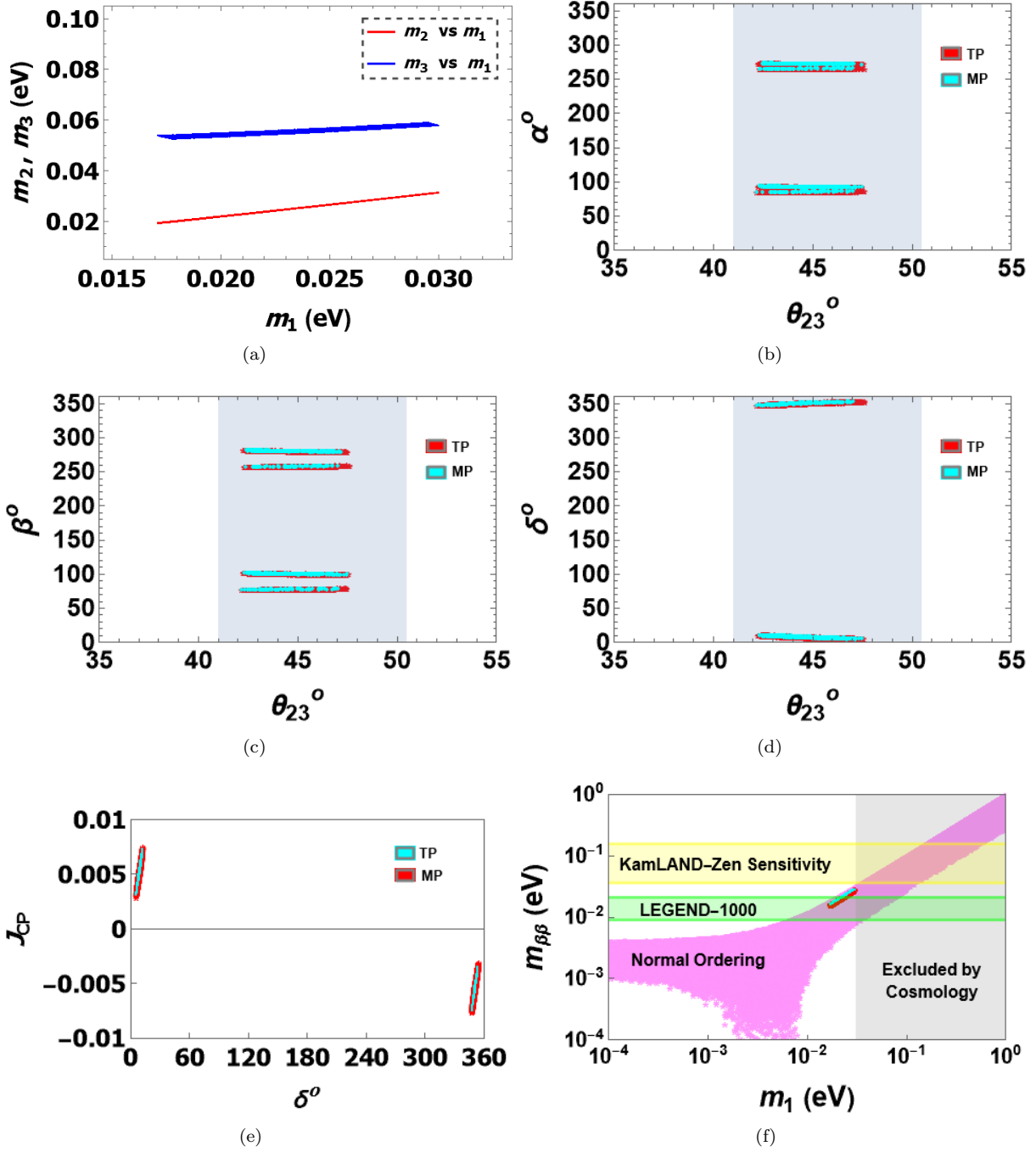


Figure 2: Shows the correlation plots between (a) m_1 vs m_2 and m_3 . (b) α vs θ_{23} . (c) β vs θ_{23} . (d) δ vs θ_{23} . (e) J_{CP} vs δ . (f) m_1 vs $m_{\beta\beta}$. The light blue strip represents the 3σ bound of θ_{23} . The red data points signify texture prediction (TP) while the blue ones signify the corrections from model sector (MP).

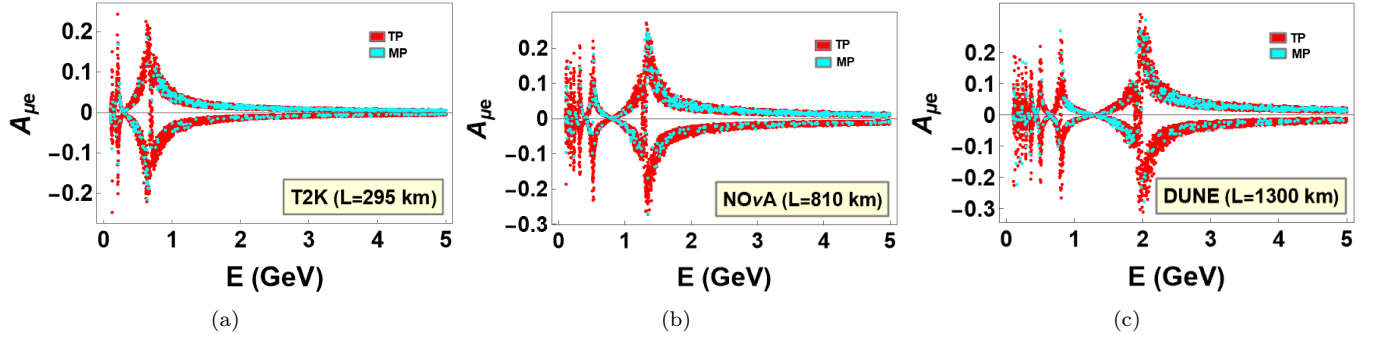


Figure 3: Shows the correlation plots between (a) $A_{\mu e}$ vs E for T2K ($L = 295$ km). (b) $A_{\mu e}$ vs E for NO ν A ($L = 810$ km). (c) $A_{\mu e}$ vs E for DUNE ($L = 1300$ km). The red data points signify texture prediction (TP) while the blue ones signify the corrections from model sector(MP).

3.2. CP Asymmetry Parameter

The effect of leptonic Dirac CP violation δ on neutrino oscillation can be studied through CP asymmetry parameter ($A_{\mu e}$). The said parameter can be expressed as shown in the following,

$$A_{\mu e} = \frac{P(\nu_\mu \rightarrow \nu_e) - P(\bar{\nu}_\mu \rightarrow \bar{\nu}_e)}{P(\nu_\mu \rightarrow \nu_e) + P(\bar{\nu}_\mu \rightarrow \bar{\nu}_e)}.$$

The transition probability $P(\nu_\mu \rightarrow \nu_e)$ can be expressed in terms of the physical parameters [36] as shown below,

$$P(\nu_\mu \rightarrow \nu_e) = P_{\text{atm}} + P_{\text{sol}} + 2\sqrt{P_{\text{atm}}}\sqrt{P_{\text{sol}}}\cos(\Delta_{ij} + \delta),$$

where, $\Delta_{ij} = \Delta m_{ij}^2 \frac{L}{4E}$. The E represents neutrino beam energy and L stands for baseline length. The quantities P_{atm} and P_{sol} can be expressed as shown below,

$$P_{\text{atm}} = \sin \theta_{23} \sin 2\theta_{13} \frac{\sin(\Delta_{31} - aL)}{(\Delta_{31} - aL)} \Delta_{31},$$

$$P_{\text{sol}} = \cos \theta_{23} \sin 2\theta_{12} \frac{\sin(aL)}{(aL)} \Delta_{21}.$$

The parameter $a = G_F N_e / \sqrt{2}$ depends on the medium through which the neutrino propagates and arises due to matter effects in neutrino propagation through the Earth. The factor G_F stands for the Fermi constant and N_e represents the electron number density of the medium. For the earth, a is approximately 3500km^{-1} [36]. The CP asymmetry parameter can be expressed in terms of the physical parameters as shown below,

$$A_{\mu e} = \frac{2\sqrt{P_{\text{atm}}}\sqrt{P_{\text{sol}}}\sin \Delta_{32} \sin \delta}{P_{\text{atm}} + 2\sqrt{P_{\text{atm}}}\sqrt{P_{\text{sol}}}\cos \Delta_{32} \cos \delta + P_{\text{sol}}}.$$

In the present work, we study the CP asymmetry parameter in the light of three experiments with different baseline lengths: T2K ($L = 295$ km), NO ν A ($L = 810$ km) and DUNE ($L = 1300$ km) (see Figs. 3(a)-3(c)). For the above analysis, the beam energy E is set at (0.5 – 5) GeV.

For the above numerical analysis, the variation of the texture parameters are shown in Fig. (4). We wish to state that the information on the texture parameters will be helpful while connecting the texture and model sector. In the next section, by following a top-down approach we shall try to achieve the texture from symmetry framework.

4. Symmetry Framework

In section (2), the texture is proposed in a framework neutral way and the analysis shows that it is consistent with the experimental data. In this section, we present a concrete model for the proposed neutrino mass matrix texture. It is important to note that deriving a model-independent texture within a symmetry framework is quite challenging. Ensuring the independence of the texture parameters is essential while expressing them in terms of the model parameters. To achieve this, we adopt a framework where both Type-I and Type-II seesaw mechanisms contribute.

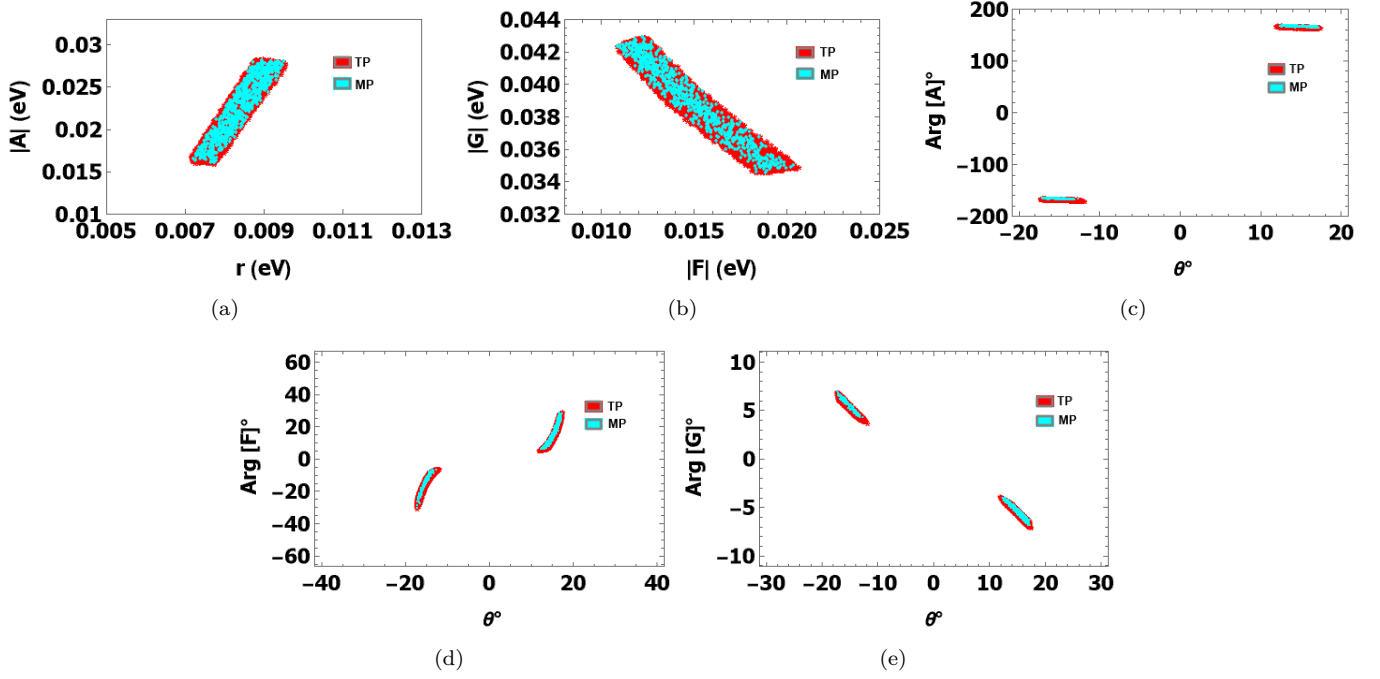


Figure 4: Shows the correlation plots between (a) $|A|$ vs r . (b) $|G|$ vs $|F|$. (c) $\text{Arg}[A]$ vs θ . (d) $\text{Arg}[F]$ vs θ . (e) $\text{Arg}[G]$ vs θ . The red data points signify texture prediction (TP) while the blue ones signify the corrections from model sector (MP).

Fields	D_{l_L}	l_R	ν_{l_R}	H	Δ	χ	ψ	ξ	η	κ
$SU(2)_L$	2	1	1	2	3	1	1	1	1	1
$U(1)_Y$	-1	(-2, -2, -2)	(0, 0, 0)	1	-2	0	0	0	0	0
A_4	3	(1, 1', 1'')	(1, 1', 1'')	3	3	1	1	1	1'	1
Z_{10}	0	(0, 0, 0)	(0, 4, 3)	0	0	6	7	0	2	3

Table 2: The transformation properties of various fields under $SU(2)_L \times U(1)_Y \times A_4 \times Z_{10}$ group.

4.1. The Yukawa Lagrangian

We start with a framework where the SM gauge group is extended to $SU(2)_L \times U(1)_Y \times A_4 \times Z_{10}$. In this regard, we extend the field content of the SM by introducing right-handed neutrinos and extra scalar fields. The transformation properties of the extended field content are summarised in Table (2). The product rules under A_4 group can be found in Appendix A. The desired Yukawa Lagrangian borne out of the said framework assumes the following form,

$$\begin{aligned}
-\mathcal{L}_Y &= y_e(\bar{D}_{l_L}H)e_R + y_\mu(\bar{D}_{l_L}H)\mu_R + y_\tau(\bar{D}_{l_L}H)\tau_R + y_1(\bar{D}_{l_L}\tilde{H})\nu_{eR} + \frac{y_2}{\Lambda} \\
&\quad (\bar{D}_{l_L}\tilde{H})\nu_{\mu R}\chi + \frac{y_3}{\Lambda}(\bar{D}_{l_L}\tilde{H})\nu_{\tau R}\psi + \frac{y_a}{2}(\bar{\nu}_{eR}^c\nu_{eR})\xi + \frac{y_b}{2}[(\bar{\nu}_{\mu R}^c\nu_{\tau R}) \\
&\quad + (\bar{\nu}_{\tau R}^c\nu_{\mu R})]\xi\kappa + \frac{y_c}{2}(\bar{\nu}_{\mu R}^c\nu_{\mu R})\eta + y_{T_2}(\bar{D}_{l_L}D_{l_L}^c) i\tau^2\Delta + h.c., \tag{2}
\end{aligned}$$

where, Λ is the cut-off scale of the theory. The Lagrangian is constructed in leading order. The presence of Z_{10} [37] in the model restricts the undesirable terms that are permitted by A_4 . Keeping in mind the targeted neutrino mass matrix in Eq. (1), the vacuum expectation values (vev) for the scalar fields are chosen as: $\langle H \rangle_0 = v_H(1, 1, 1)^T$, $\langle \Delta \rangle_0 = v_\Delta(v_1, v_2, 0)^T$, $\langle \chi \rangle_0 = v_\chi$, $\langle \psi \rangle_0 = v_\psi$, $\langle \xi \rangle_0 = v_\xi$, $\langle \eta \rangle_0 = v_\eta$ and $\langle \kappa \rangle_0 = v_\kappa$ respectively. The potential that shelters the chosen vacuum alignments is discussed in subsection 4.3.

We derive the charged lepton mass matrix (M_l) as shown in the following,

$$M_l = v_H \begin{bmatrix} y_e & y_\mu & y_\tau \\ y_e & \omega y_\mu & \omega^2 y_\tau \\ y_e & \omega^2 y_\mu & \omega y_\tau \end{bmatrix},$$

We diagonalize M_l as $M_l^{diag} = U_{l_L}^\dagger M_l U_{l_R}$, where $M_l^{diag} = \sqrt{3} v_H \text{diag}(y_e, y_\mu, y_\tau)$. The U_{l_L} and U_{l_R} are expressed as shown below,

$$U_{l_L} = \frac{1}{\sqrt{3}} \begin{bmatrix} 1 & 1 & 1 \\ 1 & \omega & \omega^2 \\ 1 & \omega^2 & \omega \end{bmatrix}, \quad U_{l_R} = \text{diag}[1, 1, 1].$$

The Dirac neutrino mass matrix(M_D) and the right-handed neutrino mass matrix(M_R) are obtained as follows,

$$M_D = \begin{bmatrix} y_1 v_H & \frac{y_2}{\Lambda} v_H v_\chi & \frac{y_3}{\Lambda} v_H v_\psi \\ y_1 v_H & \frac{y_2}{\Lambda} \omega v_H v_\chi & \frac{y_3}{\Lambda} \omega^2 v_H v_\psi \\ y_1 v_H & \frac{y_2}{\Lambda} \omega^2 v_H v_\chi & \frac{y_3}{\Lambda} \omega v_H v_\psi \end{bmatrix}, \quad M_R = \begin{bmatrix} \frac{y_a}{2} v_\xi & 0 & 0 \\ 0 & \frac{y_c}{2} v_\eta & \frac{y_b}{2} v_\xi v_\kappa \\ 0 & \frac{y_b}{2} v_\xi v_\kappa & 0 \end{bmatrix}.$$

We take the Type-I and Type-II contributions and construct the light neutrino mass matrix (M_{ν_s}) in the basis where M_l is non-diagonal

$$M_{\nu_s} = -M_D M_R^{-1} M_D^T + \begin{bmatrix} 0 & 0 & y_{T_2} v_1 \\ 0 & 0 & y_{T_2} v_2 \\ y_{T_2} v_1 & y_{T_2} v_2 & 0 \end{bmatrix}.$$

On redefining the above neutrino mass matrix in a basis where M_l is diagonal, we obtain the final neutrino mass matrix following the transformation: $M_\nu = U_{l_L}^T M_{\nu_s} U_{l_L}$ as shown below,

$$M_\nu = \begin{bmatrix} -\frac{6v^2 y_1^2}{y_a v_\xi} + \frac{2v_1 y_T}{3} + \frac{2v_2 y_T}{3} & \frac{y_T}{3} \sqrt{v_1^2 - v_2 v_1 + v_2^2} e^{i\phi} & \frac{y_T}{3} \sqrt{v_1^2 - v_2 v_1 + v_2^2} e^{-i\phi} \\ \frac{y_T}{3} \sqrt{v_1^2 - v_2 v_1 + v_2^2} e^{i\phi} & \frac{6v^2 y_3^2 y_c v_\eta v_\psi^2}{\Lambda^2 y_b^2 v_\kappa^2 v_\xi^2} + y_T \left(\frac{2v_2}{3} - \frac{v_1}{3} - \frac{iv_1}{\sqrt{3}} \right) & -\frac{6v^2 y_2 y_3 v_\chi v_\psi}{\Lambda^2 y_b v_\kappa v_\xi} - \frac{y_T}{3} (v_1 + v_2) \\ \frac{y_T}{3} \sqrt{v_1^2 - v_2 v_1 + v_2^2} e^{-i\phi} & -\frac{6v^2 y_2 y_3 v_\chi v_\psi}{\Lambda^2 y_b v_\kappa v_\xi} - \frac{v_1 y_T}{3} - \frac{v_2 y_T}{3} & \frac{2y_T}{3} \sqrt{v_1^2 - v_2 v_1 + v_2^2} e^{i\phi} \end{bmatrix}, \quad (3)$$

where, $\phi = -\tan^{-1} [\sqrt{3}v_1/(v_1 - 2v_2)]$. The above model enhanced mass matrix carrying *sixteen* model parameters involving eight vevs, seven Yukawa couplings and the cut-off scale, resembles the exact form of the neutrino mass matrix texture expressed in terms of r, θ, A, F and G as presented in Eq. (1). It's worth mentioning that the independence of the texture parameters are maintained while expressing them in terms of the model parameters.

The given model incorporates several scalar fields, which play a crucial role in maintaining the independence of the texture parameters. In addition, to cut short certain terms from the right-handed neutrino mass matrix (M_R), we introduce some extra scalar fields in our model. This step is necessary to enhance the efficiency of the model. In the next section, we shall try to relate the parameters from texture and model sector.

4.2. Important Relations

We highlight that, in order to obtain the proposed texture as shown in Eq. (1) from symmetry, the v_1 and v_2 must be real. In addition, the desired texture demands Yukawa coupling y_T as positive. For integrity, the numerical values of the individual model parameters are needed to be recognised. However, this task is challenging. However, we obtain some useful relations among the model and texture parameters as shown below,

$$\frac{v_1}{v_2} = 2 - \frac{6b_1}{3b_1 + \sqrt{3}b_2}, \quad (4)$$

$$\frac{v_\chi^2}{v_\eta} = \frac{\Lambda^2 y_c (b_1 + \sqrt{3}b_2 - g)^2}{6v^2 y_2^2 (2b_1 - 2ib_2 + f)}, \quad (5)$$

$$v_\xi = -\frac{6\sqrt{3}v^2 y_1^2}{\sqrt{3}ay_a + 2\sqrt{3}b_1 y_a + 6b_2 y_a}, \quad (6)$$

where, $b_1 = r \cos \theta$ and $b_2 = r \sin \theta$. We expect that these relations, somehow, will help to understand the numerical domain of the model parameters more closely. The parameter space of the elements, $v_1/v_2, |v_\chi^2/v_\eta|$ and $|v_\xi|$ are presented in Fig. 5). For this, we allow the cut-off scale and the Yukawa couplings to vary randomly in the bounds: $(10^3 - 10^{16})$ GeV and $(0.01 - 0.99)$ respectively. Needless to mention, the v_H is taken as 246 GeV.

We mention that the relations appearing in Eqs. (4)-(6) are solely obtained from the Yukawa sector. However, the vevs that appear there, are solely connected to the scalar sector, which will be addressed in the next section.

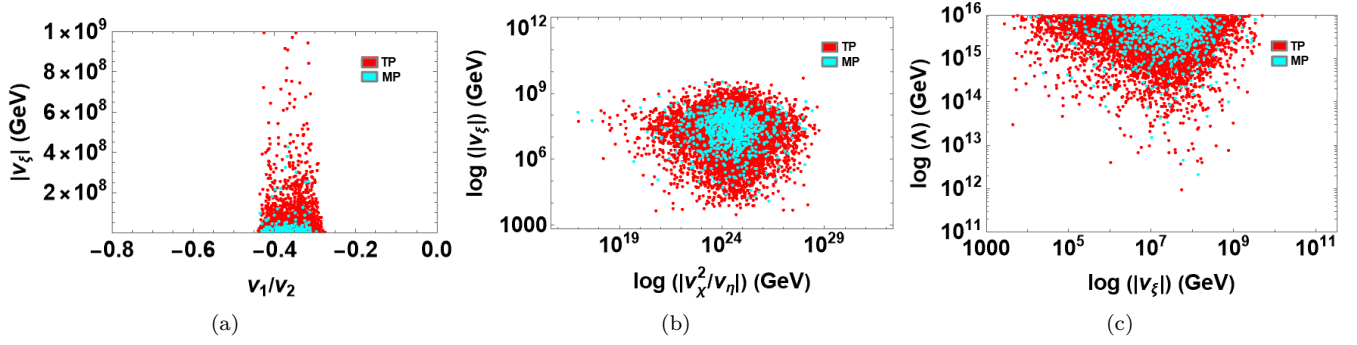


Figure 5: Shows the correlation plots between (a) v_1/v_2 vs $|v_\xi|$. (b) $\log(|v_\xi|)$ vs $\log(|v_\chi^2/v_\eta|)$. (c) $\log(\Lambda)$ vs $\log(|v_\xi|)$. The red points signify texture prediction (TP) while the blue data points signify the corrections from model sector(MP).

4.3. The Scalar Sector

There are seven complex scalar fields in the model and, the associated $SU(2)_L \times U(1)_Y \times A_4 \times Z_{10}$ invariant potential, is shown explicitly in Appendix B. We see that there are seven μ^2 's and fifty one λ 's in the potential expression. Thus it enhances the liberty to choose the desired vacuum alignments for the scalar fields. The eleven minimisation conditions in support of the vacuum alignments as discussed in section 4.1 are elaborated in Appendix B.

From the minimization conditions, we get the expression for μ_Δ^2 as shown below,

$$\begin{aligned} \mu_\Delta^2 = & \frac{1}{v_2}(-2\mu v_H^2 - 2\lambda_3^{H\Delta} v_H^2 v_1 - 2\lambda_4^{H\Delta} v_H^2 v_1 - 3\lambda_1^{H\Delta} v_H^2 v_2 + i(\sqrt{3}\lambda_2^\Delta v_1^2 v_2 \\ & - \sqrt{3}\lambda_2^\Delta v_2^3) - 2\lambda_1^\Delta v_1^2 v_2 + \lambda_2^\Delta v_1^2 v_2 - 4\lambda_3^\Delta v_1^2 v_2 - 2\lambda_4^\Delta v_1^2 v_2 - 2\lambda_1^\Delta v_2^3 \\ & + \lambda_2^\Delta v_2^3 - \lambda_1^{\Delta\eta} v_2 v_\eta^2 - \lambda_1^{\Delta\kappa} v_2 v_\kappa^2 - \lambda_1^{\Delta\xi} v_2 v_\xi^2 - \lambda_1^{\Delta\chi} v_2 v_\chi^2 - \lambda_1^{\Delta\psi} v_2 v_\psi). \end{aligned}$$

As v_1 and v_2 are real in our model, it is evident from the above expression that μ_Δ^2 is complex quantity. In order to restrict this, we have only one choice i.e., $\lambda_2^\Delta = 0$. In addition, we obtain the following significant relations:

$$\lambda_4^{H\Delta} = \frac{3}{4}\lambda_2^{H\Delta} \left(\frac{1}{\left(\frac{v_1}{v_2}\right)^2} + \left(\frac{v_1}{v_2}\right) - \frac{2}{\left(\frac{v_1}{v_2}\right)} + 1 \right), \quad (7)$$

$$\mu v_2 = \frac{2\lambda_3^{H\Delta} \left(\left(\frac{v_1}{v_2}\right)^2 - \left(\frac{v_1}{v_2}\right) + 1 \right)}{\left(\frac{v_1}{v_2}\right)^2 - 3\left(\frac{v_1}{v_2}\right) - \frac{1}{\left(\frac{v_1}{v_2}\right)} + 2}, \quad (8)$$

$$\left(\frac{v}{v_2}\right)^2 = \frac{2\left(\frac{v_1}{v_2}\right)^3 \left(\lambda_4^\Delta + 2\lambda_3^\Delta \left(\left(\frac{v_1}{v_2}\right)^2 - 1 \right) + \lambda_4^\Delta \left(\frac{v_1}{v_2}\right)^2 \right)}{3\lambda_2^{H\Delta} \left(1 + \left(\frac{v_1}{v_2}\right) \left(\left(\frac{v_1}{v_2}\right) \left(\left(\frac{v_1}{v_2}\right)^3 - 2\left(\frac{v_1}{v_2}\right) + 4 \right) - 3 \right) \right)}. \quad (9)$$

The above relations are significant in the sense that those are expressible in terms of v_1/v_2 , which, in turn, is dictated by the texture parameters r and θ (see Eq. (4)). In the next section, we shall see how these relations will help us to curtail the parameter space.

4.4. Refined Parameter Space

We first try to realize the parameter domain of the elements : $\lambda_4^{H\Delta}$, μv_2 and $(v/v_2)^2$ which depend on the free parameters λ_3^Δ , λ_4^Δ , $\lambda_2^{H\Delta}$, $\lambda_4^{H\Delta}$ and v_1/v_2 . The parameter v_1/v_2 is guided by r and θ . From the phenomenological analysis in section 2, we are aware of the parameter space of the two said texture parameters. Moreover, we adhere to the fact that the quartic coupling constants, $\lambda \sim \mathcal{O}(1)$. Motivated by this, we allow the free parameters $\lambda_3^{H\Delta}$, λ_3^Δ , λ_4^Δ to vary in the range (0.01 – 0.99). With these inputs, we graphically visualise the parameter space of $\lambda_4^{H\Delta}$, μv_2 and $(v/v_2)^2$ in Figs. (6). We further extend the analysis to gain deeper insight of domain of v_1 , v_2 and μ (see Fig. (7)).

Our model requires, $(v/v_2)^2 > 0$ and the reality condition demands $\lambda_4^{H\Delta} \lesssim 1$. It is interesting to note that on incorporating these two constraints, the parameter space of $(v/v_2)^2$ is restricted to a narrow region (this is shown in

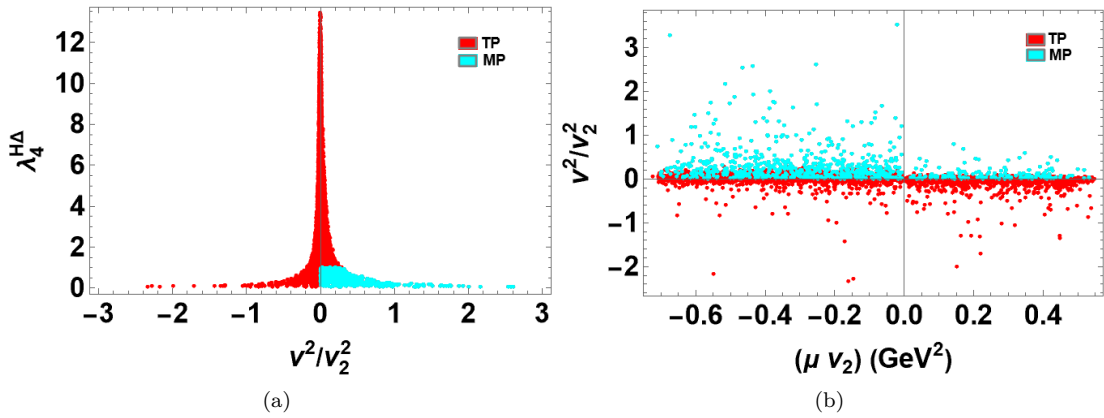


Figure 6: Shows the correlation plots between (a) $\lambda_4^{H\Delta}$ vs v^2/v_2^2 . (b) v^2/v_2^2 vs μv_2 . The red data points signify texture prediction (TP) while the blue ones signify the corrections from model sector(MP).

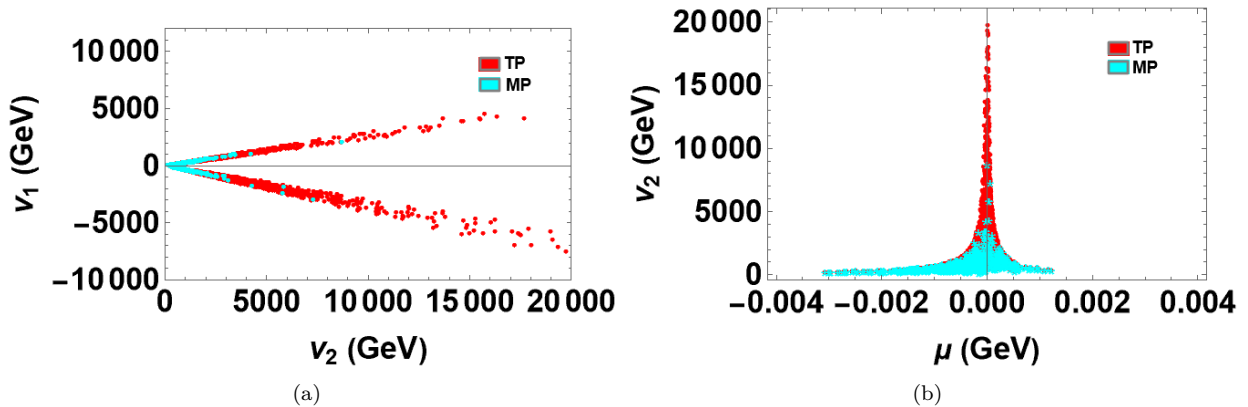


Figure 7: Shows the correlation plots between (a) v_1 vs v_2 . (b) v_2 vs μ . The red data points signify texture prediction (TP) while the blue ones signify the corrections from model sector(MP).

blue in Fig. (6(a))). This refinement is not confined only to the said parameter, rather transmits to the parameter space of v_1 , v_2 and μ (see Fig. (7)).

When we study a texture from a model independent point of view, the parameter space of the observable is quite wide in comparison to the scenario where the former is achieved following a top-down route. This is because the model parameters are subjected to many restrictions. One such scenario is discussed in the earlier paragraph. Thus, the refinement of the model parameters will also affect the predictions of the observables discussed earlier. We revisit the graphical analysis in sections 3-4 and highlight the filtered data points in blue (see Figs. (2)-(5)). In the next section, we shall conclude.

5. Summary and Discussion

The study of neutrino mass matrix texture has been explored exhaustively by the model builders. At the same time, the experiments are gradually achieving more precise predictions, whereas the fundamental issues such as the neutrino mass hierarchy and anomalies related to physical parameters remain unresolved. Hence, there lies the importance of looking into more predictive textures of neutrino mass matrix both from a bottom-up and top-down perspective. Although physics is independent of parametrization, yet a meaningful parametrization may simplify a certain problem and thereby will help to approach a framework in a better way. With this motivation, the present piece of work adapts “Exponential parametrization”, where the general neutrino mass matrix element is visualised in polar form. We have posited a neutrino mass matrix texture under the roof of the said parametrisation which is quite promising in the light of neutrino oscillation experiments. We predict narrow bound/ allowed and forbidden regions for the observable parameters like atmospheric angle and three CP violating phases. The texture is perfectly obtained in its exact form ensuring the independence of the parameters, in a discrete symmetry based framework. Moreover in this work, we have emphasized on how accurately the texture is consistent with the model in terms of refined parameter space.

It is important to mention that a similar approach encompassing texture analysis and preference for certain parametrization may also assist us in exploring both quark and lepton sectors in the unified frameworks.

Acknowledgements

The research work of PC is supported by Innovation in Science Pursuit for Inspired Research (INSPIRE), Department of Science and Technology, Government of India, New Delhi vide grant No. IF190651.

Appendix A. Product Rules of A_4

The discrete group A_4 is a subgroup of $SU(3)$ and has 12 elements. The group has four irreducible representation out of which three are one dimensional and one is three dimensional. In S-basis, the product of two triplets gives,

$$3 \times 3 = 1 + 1' + 1'' + 3_S + 3_A, \quad (\text{A.1})$$

where,

$$1 = (a_1 \bar{b}_1 + a_2 \bar{b}_2 + a_3 \bar{b}_3) \quad (\text{A.2})$$

$$1' = (a_1 \bar{b}_1 + \omega^2 a_2 \bar{b}_2 + \omega a_3 \bar{b}_3) \quad (\text{A.3})$$

$$1'' = (a_1 \bar{b}_1 + \omega a_2 \bar{b}_2 + \omega^2 a_3 \bar{b}_3) \quad (\text{A.4})$$

$$(3 \times 3)_S = \begin{bmatrix} a_2 b_3 + a_3 b_2 \\ a_3 b_1 + a_1 b_3 \\ a_1 b_2 + a_2 b_1 \end{bmatrix}, \quad (\text{A.5})$$

$$(3 \times 3)_A = \begin{bmatrix} a_2 b_3 - a_3 b_2 \\ a_3 b_1 - a_1 b_3 \\ a_1 b_2 - a_2 b_1 \end{bmatrix}. \quad (\text{A.6})$$

The trivial singlet can be obtained from the following singlet product rules,

$$1 \times 1 = 1, \quad 1' \times 1'' = 1, \quad 1'' \times 1' = 1. \quad (\text{A.7})$$

Appendix B. The Scalar Potential

To justify the vacuum alignments of the scalar fields, we construct the $SU(2)_L \times U(1)_Y \times A_4 \times Z_{10}$ invariant scalar potential in the following way,

$$\begin{aligned} V = & V(H) + V(\Delta) + V(\chi) + V(\psi) + V(\xi) + V(\eta) + V(\kappa) + V(H, \Delta) + V(H, \chi) + V(H, \psi) + V(H, \xi) \\ & + V(H, \eta) + V(H, \kappa) + V(\Delta, \chi) + V(\Delta, \psi) + V(\Delta, \xi) + V(\Delta, \eta) + V(\Delta, \kappa) + V(\chi, \psi) + V(\chi, \xi) \\ & + V(\chi, \eta) + V(\chi, \kappa) + V(\psi, \xi) + V(\psi, \eta) + V(\psi, \kappa) + V(\xi, \eta) + V(\xi, \kappa) + V(\eta, \kappa). \end{aligned} \quad (\text{B.1})$$

The explicit forms of the terms appearing in the scalar potential are given by,

$$V(H) = \mu_H^2 (H^\dagger H) + \lambda_1^H (H^\dagger H)(H^\dagger H) + \lambda_2^H (H^\dagger H)_{1'} (H^\dagger H)_{1''} + \lambda_3^H (H^\dagger H)_{3_s} (H^\dagger H)_{3_s} + \lambda_4^H (H^\dagger H)_{3_s} (H^\dagger H)_{3_a} + \lambda_5^H (H^\dagger H)_{3_a} (H^\dagger H)_{3_a}, \quad (\text{B.2})$$

$$V(\Delta) = \mu_\Delta^2 Tr(\Delta^\dagger \Delta) + \lambda_1^\Delta Tr(\Delta^\dagger \Delta) Tr(\Delta^\dagger \Delta) + \lambda_2^\Delta Tr(\Delta^\dagger \Delta)_{1'} Tr(\Delta^\dagger \Delta)_{1''} + \lambda_3^\Delta Tr(\Delta^\dagger \Delta)_{3_s} Tr(\Delta^\dagger \Delta)_{3_s} + \lambda_4^\Delta Tr(\Delta^\dagger \Delta)_{3_s} Tr(\Delta^\dagger \Delta)_{3_a} + \lambda_5^\Delta Tr(\Delta^\dagger \Delta)_{3_a} Tr(\Delta^\dagger \Delta)_{3_a}, \quad (\text{B.3})$$

$$V(\chi) = \mu_\chi^2 (\chi^\dagger \chi) + \lambda^\chi (\chi^\dagger \chi)(\chi^\dagger \chi), \quad (\text{B.4})$$

$$V(\psi) = \mu_\psi^2 (\psi^\dagger \psi) + \lambda^\psi (\psi^\dagger \psi)(\psi^\dagger \psi), \quad (\text{B.5})$$

$$V(\xi) = \mu_\xi^2 (\xi^\dagger \xi) + \lambda^\xi (\xi^\dagger \xi)(\xi^\dagger \xi), \quad (\text{B.6})$$

$$V(\eta) = \mu_\eta^2 (\eta^\dagger \eta) + \lambda^\eta (\eta^\dagger \eta)(\eta^\dagger \eta), \quad (\text{B.7})$$

$$V(\kappa) = \mu_\kappa^2 (\kappa^\dagger \kappa) + \lambda^\kappa (\kappa^\dagger \kappa)(\kappa^\dagger \kappa), \quad (\text{B.8})$$

$$\begin{aligned}
V(H, \Delta) &= \lambda_1^{H\Delta}(H^\dagger H)Tr(\Delta^\dagger \Delta) + \lambda_2^{H\Delta}[(H^\dagger H)_{1'}Tr(\Delta^\dagger \Delta)_{1''} + (H^\dagger H)_{1''}Tr(\Delta^\dagger \Delta)_{1'}] + \lambda_3^{H\Delta}(H^\dagger H)_{3_s} \\
&\quad Tr(\Delta^\dagger \Delta)_{3_s} + \lambda_4^{H\Delta}[(H^\dagger H)_{3_s}Tr(\Delta^\dagger \Delta)_{3_a} + (H^\dagger H)_{3_a}Tr(\Delta^\dagger \Delta)_{3_s}] + \lambda_5^{H\Delta}(H^\dagger H)_{3_a} \\
&\quad Tr(\Delta^\dagger \Delta)_{3_a} + \mu(H^T i\sigma_2 \Delta^\dagger H), \tag{B.9}
\end{aligned}$$

$$V(H, \chi) = \lambda_1^{H\chi}(H^\dagger H)(\chi^\dagger \chi), \tag{B.10}$$

$$V(H, \psi) = \lambda_1^{H\psi}(H^\dagger H)(\psi^\dagger \psi), \tag{B.11}$$

$$V(H, \xi) = \lambda_1^{H\xi}(H^\dagger H)(\xi^\dagger \xi), \tag{B.12}$$

$$V(H, \eta) = \lambda_1^{H\eta}(H^\dagger H)(\eta^\dagger \eta), \tag{B.13}$$

$$V(H, \kappa) = \lambda_1^{H\kappa}(H^\dagger H)(\kappa^\dagger \kappa), \tag{B.14}$$

$$V(\Delta, \chi) = \lambda_1^{\Delta\chi}Tr(\Delta^\dagger \Delta)(\chi^\dagger \chi), \tag{B.15}$$

$$V(\Delta, \psi) = \lambda_1^{\Delta\psi}Tr(\Delta^\dagger \Delta)(\psi^\dagger \psi), \tag{B.16}$$

$$V(\Delta, \xi) = \lambda_1^{\Delta\xi}Tr(\Delta^\dagger \Delta)(\xi^\dagger \xi), \tag{B.17}$$

$$V(\Delta, \eta) = \lambda_1^{\Delta\eta}Tr(\Delta^\dagger \Delta)(\eta^\dagger \eta), \tag{B.18}$$

$$V(\Delta, \kappa) = \lambda_1^{\Delta\kappa}Tr(\Delta^\dagger \Delta)(\kappa^\dagger \kappa), \tag{B.19}$$

$$V(\chi, \psi) = \lambda_1^{\chi\psi}(\chi^\dagger \chi)(\psi^\dagger \psi), \tag{B.20}$$

$$V(\chi, \xi) = \lambda_1^{\chi\xi}(\chi^\dagger \chi)(\xi^\dagger \xi), \tag{B.21}$$

$$V(\chi, \eta) = \lambda_1^{\chi\eta}(\chi^\dagger \chi)(\eta^\dagger \eta), \tag{B.22}$$

$$V(\chi, \kappa) = \lambda_1^{\chi\kappa}(\chi^\dagger \chi)(\kappa^\dagger \kappa), \tag{B.23}$$

$$V(\psi, \xi) = \lambda_1^{\psi\xi}(\psi^\dagger \psi)(\xi^\dagger \xi), \tag{B.24}$$

$$V(\psi, \eta) = \lambda_1^{\psi\eta}(\psi^\dagger \psi)(\eta^\dagger \eta), \tag{B.25}$$

$$V(\psi, \kappa) = \lambda_1^{\psi\kappa}(\psi^\dagger \psi)(\kappa^\dagger \kappa), \tag{B.26}$$

$$V(\xi, \eta) = \lambda_1^{\xi\eta}(\xi^\dagger \xi)(\eta^\dagger \eta), \tag{B.27}$$

$$V(\xi, \kappa) = \lambda_1^{\xi\kappa}(\xi^\dagger \xi)(\kappa^\dagger \kappa), \tag{B.28}$$

$$V(\eta, \kappa) = \lambda_1^{\eta\kappa}(\eta^\dagger \eta)(\kappa^\dagger \kappa). \tag{B.29}$$

Without loss of generality, the following equations are valid from the minimisation conditions of the scalar potential for the chosen vacuum alignments: $\langle H \rangle_0 = v_H(1, 1, 1)^T$, $\langle \Delta \rangle_0 = v_\Delta(v_1, v_2, 0)^T$, $\langle \chi \rangle_0 = v_\chi$, $\langle \psi \rangle_0 = v_\psi$, $\langle \xi \rangle_0 = v_\xi$, $\langle \eta \rangle_0 = v_\eta$ and $\langle \kappa \rangle_0 = v_\kappa$,

$$\begin{aligned}
v_H(\mu_H^2 + v_H^2(6\lambda_1^H + 8\lambda_3^H)) + v_1^2(\lambda_1^{H\Delta} + 2\lambda_2^{H\Delta}) + 2v_1v_2(\lambda_3^{H\Delta} - \lambda_4^{H\Delta}) + v_2(2\mu + \lambda_1^{H\Delta}v_2 \\
- \lambda_2^{H\Delta}v_2) + \lambda_1^{H\eta}v_\eta^2 + \lambda_1^{H\kappa}v_\kappa^2 + \lambda_1^{H\xi}v_\xi^2 + \lambda_1^{H\chi}v_\chi^2 + \lambda_1^{H\psi}v_\psi^2 = 0, \tag{B.30}
\end{aligned}$$

$$\begin{aligned}
v_H(\mu_H^2 + v_H^2(6\lambda_1^H + 8\lambda_3^H)) + v_1^2(\lambda_1^{H\Delta} - \lambda_2^{H\Delta}) + 2v_1v_2(\lambda_3^{H\Delta} + \lambda_4^{H\Delta}) + v_2^2(\lambda_1^{H\Delta} + 2\lambda_2^{H\Delta}) \\
+ \lambda_1^{H\eta}v_\eta^2 + \lambda_1^{H\kappa}v_\kappa^2 + \lambda_1^{H\xi}v_\xi^2 + \lambda_1^{H\chi}v_\chi^2 + \lambda_1^{H\psi}v_\psi^2 = 0 \tag{B.31}
\end{aligned}$$

$$\begin{aligned}
v_H(\mu_H^2 + v_H^2(6\lambda_1^H + 8\lambda_3^H)) + (\lambda_1^{H\Delta} - \lambda_2^{H\Delta})(v_1^2 + v_2^2) + 2\mu v_1 + \lambda_1^{H\eta}v_\eta^2 + \lambda_1^{H\kappa}v_\kappa^2 + \lambda_1^{H\xi}v_\xi^2 + \\
\lambda_1^{H\chi}v_\chi^2 + \lambda_1^{H\psi}v_\psi^2 = 0, \tag{B.32}
\end{aligned}$$

$$\begin{aligned}
v_H^2(3\lambda_1^{H\Delta}v_1 + 2(\mu + \lambda_3^{H\Delta}v_2 - \lambda_4^{H\Delta}v_2)) + v_1(\mu_\Delta^2 + 2\lambda_1^\Delta v_1^2 + 2v_2^2(\lambda_1^\Delta + 2\lambda_3^\Delta - \lambda_4^\Delta) + \lambda_1^{\Delta\eta}v_\eta^2 \\
+ \lambda_1^{\Delta\kappa}v_\kappa^2 + \lambda_1^{\Delta\xi}v_\xi^2 + \lambda_1^{\Delta\chi}v_\chi^2 + \lambda_1^{\Delta\psi}v_\psi^2) = 0, \tag{B.33}
\end{aligned}$$

$$\begin{aligned}
v_H^2(2(\mu + v_1(\lambda_3^{H\Delta} + \lambda_4^{H\Delta})) + 3\lambda_1^{H\Delta}v_2) + v_2(\mu_\Delta^2 + 2v_1^2(\lambda_1^\Delta + 2\lambda_3^\Delta + \lambda_4^\Delta) + 2\lambda_1^{\Delta\eta}v_\eta^2 \\
+ \lambda_1^{\Delta\kappa}v_\kappa^2 + \lambda_1^{\Delta\xi}v_\xi^2 + \lambda_1^{\Delta\chi}v_\chi^2 + \lambda_1^{\Delta\psi}v_\psi^2) = 0, \tag{B.34}
\end{aligned}$$

$$2v_H^2(\mu + v_1(\lambda_3^{H\Delta} - \lambda_4^{H\Delta}) + v_2(\lambda_3^{H\Delta} + \lambda_4^{H\Delta})) = 0, \tag{B.35}$$

$$v_\chi(\mu_\chi^2 + 3\lambda_1^{H\chi}v_H^2 + \lambda_1^{\Delta\chi}(v_1^2 + v_2^2) + \lambda_1^{\chi\eta}v_\eta^2 + \lambda_1^{\chi\kappa}v_\kappa^2 + \lambda_1^{\chi\xi}v_\xi^2 + 2\lambda_1^\chi v_\chi^2 + \lambda_1^{\chi\psi}v_\psi^2) = 0, \quad (\text{B.36})$$

$$v_\psi(\mu_\psi^2 + 3\lambda_1^{H\psi}v_H^2 + \lambda_1^{\Delta\psi}(v_1^2 + v_2^2) + \lambda_1^{\psi\eta}v_\eta^2 + \lambda_1^{\psi\kappa}v_\kappa^2 + \lambda_1^{\psi\xi}v_\xi^2 + \lambda_1^{\chi\psi}v_\chi^2 + 2\lambda_\psi v_\psi^2) = 0, \quad (\text{B.37})$$

$$v_\xi(\mu_\xi^2 + 3\lambda_1^{H\xi}v_H^2 + \lambda_1^{\Delta\xi}(v_1^2 + v_2^2) + \lambda_1^{\xi\eta}v_\eta^2 + \lambda_1^{\xi\kappa}v_\kappa^2 + 2\lambda_\xi v_\xi^2 + \lambda_1^{\chi\xi}v_\chi^2 + \lambda_1^{\psi\xi}v_\psi^2) = 0, \quad (\text{B.38})$$

$$v_\eta(\mu_\eta^2 + 2\lambda_1^{\Delta\eta}(v_1^2 + v_2^2) + 2\lambda^\eta v_\eta^2 + \lambda_1^{\eta\kappa}v_\kappa^2 + \lambda_1^{\xi\eta}v_\xi^2 + \lambda_1^{\chi\eta}v_\chi^2 + \lambda_1^{\psi\eta}v_\psi^2 + 3\lambda_1^{H\eta}v_H^2) = 0, \quad (\text{B.39})$$

$$v_\kappa(\mu_\kappa^2 + 2\lambda_1^{\Delta\kappa}(v_1^2 + v_2^2) + \lambda_1^{\eta\kappa}v_\eta^2 + 2\lambda^\kappa v_\kappa^2 + \lambda_1^{\xi\kappa}v_\xi^2 + \lambda_1^{\chi\kappa}v_\chi^2 + \lambda_1^{\psi\kappa}v_\psi^2 + 3\lambda_1^{H\kappa}v_H^2) = 0. \quad (\text{B.40})$$

References

- [1] B. Pontecorvo, Mesonium and anti-mesonium, *Sov. Phys. JETP* 6 (1957) 429.
- [2] S. L. Glashow, Partial Symmetries of Weak Interactions, *Nucl. Phys.* 22 (1961) 579–588. doi:10.1016/0029-5582(61)90469-2.
- [3] S. Weinberg, A Model of Leptons, *Phys. Rev. Lett.* 19 (1967) 1264–1266. doi:10.1103/PhysRevLett.19.1264.
- [4] A. Salam, Weak and Electromagnetic Interactions, *Conf. Proc. C* 680519 (1968) 367–377. doi:10.1142/9789812795915_0034.
- [5] M. Yoshimura, Unified Gauge Theories and the Baryon Number of the Universe, *Phys. Rev. Lett.* 41 (1978) 281–284, [Erratum: *Phys.Rev.Lett.* 42, 746 (1979)]. doi:10.1103/PhysRevLett.41.281.
- [6] E. K. Akhmedov, G. C. Branco, M. N. Rebelo, Seesaw mechanism and structure of neutrino mass matrix, *Phys. Lett. B* 478 (2000) 215–223. arXiv:hep-ph/9911364, doi:10.1016/S0370-2693(00)00282-3.
- [7] J. Schechter, J. W. F. Valle, Neutrino Masses in SU(2) x U(1) Theories, *Phys. Rev. D* 22 (1980) 2227. doi:10.1103/PhysRevD.22.2227.
- [8] J. Schechter, J. W. F. Valle, Neutrino Decay and Spontaneous Violation of Lepton Number, *Phys. Rev. D* 25 (1982) 774. doi:10.1103/PhysRevD.25.774.
- [9] P. Minkowski, $\mu \rightarrow e\gamma$ at a Rate of One Out of 10^9 Muon Decays?, *Phys. Lett. B* 67 (1977) 421–428. doi:10.1016/0370-2693(77)90435-X.
- [10] M. Gell-Mann, P. Ramond, R. Slansky, Complex Spinors and Unified Theories, *Conf. Proc. C* 790927 (1979) 315–321. arXiv:1306.4669.
- [11] R. N. Mohapatra, G. Senjanovic, Neutrino Mass and Spontaneous Parity Nonconservation, *Phys. Rev. Lett.* 44 (1980) 912. doi:10.1103/PhysRevLett.44.912.
- [12] M. Magg, C. Wetterich, Neutrino Mass Problem and Gauge Hierarchy, *Phys. Lett. B* 94 (1980) 61–64. doi:10.1016/0370-2693(80)90825-4.
- [13] G. Lazarides, Q. Shafi, C. Wetterich, Proton Lifetime and Fermion Masses in an SO(10) Model, *Nucl. Phys. B* 181 (1981) 287–300. doi:10.1016/0550-3213(81)90354-0.
- [14] I. Esteban, M. C. Gonzalez-Garcia, M. Maltoni, I. Martinez-Soler, J. a. P. Pinheiro, T. Schwetz, NuFit-6.0: updated global analysis of three-flavor neutrino oscillations, *JHEP* 12 (2024) 216. arXiv:2410.05380, doi:10.1007/JHEP12(2024)216.
- [15] P. O. Ludl, W. Grimus, A complete survey of texture zeros in the lepton mass matrices, *JHEP* 07 (2014) 090, [Erratum: *JHEP* 10, 126 (2014)]. arXiv:1406.3546, doi:10.1007/JHEP07(2014)090.

- [16] E. I. Lashin, N. Chamoun, One vanishing minor in the neutrino mass matrix, *Phys. Rev. D* 80 (2009) 093004. [arXiv:0909.2669](#), [doi:10.1103/PhysRevD.80.093004](#).
- [17] J.-Y. Liu, S. Zhou, Hybrid Textures of Majorana Neutrino Mass Matrix and Current Experimental Tests, *Phys. Rev. D* 87 (9) (2013) 093010. [arXiv:1304.2334](#), [doi:10.1103/PhysRevD.87.093010](#).
- [18] P. F. Harrison, D. H. Perkins, W. G. Scott, Tri-bimaximal mixing and the neutrino oscillation data, *Phys. Lett. B* 530 (2002) 167. [arXiv:hep-ph/0202074](#), [doi:10.1016/S0370-2693\(02\)01336-9](#).
- [19] M. Dey, P. Chakraborty, S. Roy, The μ - τ mixed symmetry and neutrino mass matrix, *Phys. Lett. B* 839 (2023) 137767, [Erratum: *Phys.Lett.B* 852, 138602 (2024)]. [arXiv:2211.01314](#), [doi:10.1016/j.physletb.2023.137767](#).
- [20] P. Chakraborty, S. Roy, The other variants of mixed μ - τ symmetry, *Nucl. Phys. B* 992 (2023) 116252. [arXiv:2304.06737](#), [doi:10.1016/j.nuclphysb.2023.116252](#).
- [21] P. Chakraborty, T. Dev, S. Roy, Two New $\mu - \tau$ Deviated Neutrino Mass Matrix Textures (4 2024). [arXiv:2404.14264](#).
- [22] P. Chakraborty, M. Dey, S. Roy, Constrained neutrino mass matrix and Majorana phases, *J. Phys. G* 51 (1) (2024) 015003. [arXiv:2202.04874](#), [doi:10.1088/1361-6471/ad074c](#).
- [23] Z. Maki, M. Nakagawa, S. Sakata, Remarks on the unified model of elementary particles, *Prog. Theor. Phys.* 28 (1962) 870–880. [doi:10.1143/PTP.28.870](#).
- [24] P. A. Zyla, et al., Review of Particle Physics, *PTEP* 2020 (8) (2020) 083C01. [doi:10.1093/ptep/ptaa104](#).
- [25] N. Aghanim, et al., Planck 2018 results. VI. Cosmological parameters, *Astron. Astrophys.* 641 (2020) A6, [Erratum: *Astron.Astrophys.* 652, C4 (2021)]. [arXiv:1807.06209](#), [doi:10.1051/0004-6361/201833910](#).
- [26] C. Jarlskog, Commutator of the Quark Mass Matrices in the Standard Electroweak Model and a Measure of Maximal CP Nonconservation, *Phys. Rev. Lett.* 55 (1985) 1039. [doi:10.1103/PhysRevLett.55.1039](#).
- [27] J. Schechter, J. W. F. Valle, Neutrinoless Double beta Decay in SU(2) x U(1) Theories, *Phys. Rev. D* 25 (1982) 2951. [doi:10.1103/PhysRevD.25.2951](#).
- [28] H. Ejiri, Neutrino-Mass Sensitivity and Nuclear Matrix Element for Neutrinoless Double Beta Decay, *Universe* 6 (12) (2020) 225. [doi:10.3390/universe6120225](#).
- [29] M. Agostini, G. Benato, J. A. Detwiler, J. Menéndez, F. Vissani, Toward the discovery of matter creation with neutrinoless $\beta\beta$ decay, *Rev. Mod. Phys.* 95 (2) (2023) 025002. [arXiv:2202.01787](#), [doi:10.1103/RevModPhys.95.025002](#).
- [30] D. Q. Adams, et al., Improved Limit on Neutrinoless Double-Beta Decay in ^{130}Te with CUORE, *Phys. Rev. Lett.* 124 (12) (2020) 122501. [arXiv:1912.10966](#), [doi:10.1103/PhysRevLett.124.122501](#).
- [31] M. Agostini, et al., Probing Majorana neutrinos with double- β decay, *Science* 365 (2019) 1445. [arXiv:1909.02726](#), [doi:10.1126/science.aav8613](#).
- [32] A. Gando, et al., Search for Majorana Neutrinos near the Inverted Mass Hierarchy Region with KamLAND-Zen, *Phys. Rev. Lett.* 117 (8) (2016) 082503, [Addendum: *Phys.Rev.Lett.* 117, 109903 (2016)]. [arXiv:1605.02889](#), [doi:10.1103/PhysRevLett.117.082503](#).
- [33] R. Arnold, et al., Measurement of the distribution of ^{207}Bi depositions on calibration sources for SuperNEMO, *JINST* 16 (07) (2021) T07012. [arXiv:2103.14429](#), [doi:10.1088/1748-0221/16/07/T07012](#).
- [34] C. Alduino, et al., Double-beta decay of ^{130}Te to the first 0^+ excited state of ^{130}Xe with CUORE-0, *Eur. Phys. J. C* 79 (9) (2019) 795. [arXiv:1811.10363](#), [doi:10.1140/epjc/s10052-019-7275-5](#).
- [35] N. Abgrall, et al., The Large Enriched Germanium Experiment for Neutrinoless $\beta\beta$ Decay: LEGEND-1000 Preconceptual Design Report (7 2021). [arXiv:2107.11462](#).
- [36] R. Sinha, P. Roy, A. Ghosal, CP transformed mixed $\mu\tau$ antisymmetry for neutrinos and its consequences, *Phys. Rev. D* 99 (3) (2019) 033009. [arXiv:1809.06615](#), [doi:10.1103/PhysRevD.99.033009](#).
- [37] M. Dey, S. Roy, Unveiling Neutrino Mysteries with $\Delta(27)$ Symmetry (9 2023). [arXiv:2309.14769](#).